Silicon (2022) 14:7991–8000
https://doi.org/10.1007/s12633-021-01567-6

ORIGINAL PAPER

Optical and Photoelectrocatalytic Properties of PbS Loaded Si Based Photocathode

L. Allad[1,2] · S. Kaci[1] · K. Benfadel[1] · D. Allam[2] · A. Ouerk[2] · A. Boukezzata[1] · C. Torki[1] · S. Anas[1] · L. Talbi[1] · Y. Ouadah[1] · S. Hocine[2] · A. Keffous[1] · S. Achacha[1] · A. Manseri[1] · S. Sam[1]

Received: 24 August 2021 / Accepted: 19 November 2021 / Published online: 3 January 2022

Abstract
Herein, we report an efficient method to produce lead sulfide PbS nanoparticle-decorated silicon (Si) pyramids arrays on a Si substrate by using pure chemical methods. A n-type nanostructured PbS thin films were prepared by chemical bath deposition onto plat Silicon (Si) and pyramid textured Silicon (SiPYs) which were derived from alkaline etching of Si substrates. The morphological characterizations were carried out by Scanning Electron Microscopy (SEM), while the optical properties were studied using Ultraviolet-Visible Spectroscopy (UV–Vis). The catalytic activity was studied by linear sweap voltammetry (LSV) in dark and under white light irradiation using potentiostat station. Cyclic voltammetry in presence and without purging CO_2 was also conducted. The LSV investigations showed the synergy effect between PbS thin films and Si for the rising and transport of the charge carriers. The results showed a higher photocatalytic towards CO_2 reduction of PbS/SiPYs compared to Silicon substrate without surface modification and sensitization. The electrode based on PbS/SiPYs/Si could efficiently be used as photocathode for the PEC reduction of CO_2 to Methanol.

Keywords PbS/SiPYs/Si · Photocathode · Thin films · Photoelectrocatalysis · CO_2RR

1 Introduction

PEC conversion of CO_2 to energetic products employing crystalline silicon Si (c-Si) as photocatalyst-based electrode have been investigated by numerous studies [1–13]. Effectively, c-Si, an indirect-gap semiconductor with a low absorption coefficient, constitute the most material used in the majority of commercial solar-driven devices, in particular, photovoltaic solar cell. However, effective capture of the incident light of silicon is therefore a non negligible stacke. In order to make use of light-trapping morphologies, structuring the surface of high-quality silicon thick wafers is the traditional technology that attracted large research interest. Thus, fabrication strategies for low dimensional morphologies such as pyramides, porous and nanowires based structures have attracted a lot of attention [14, 15]. Modifying the surfaces of silicon wafer by nanostruturation is one of the promising ways for enhancing the light harvesting since the surface-light losses are significantly reduced through photon trapping, enhancing thereby the generated current in the whole PEC process [16].

Lead sulfide (PbS) nanoparticles are interesting because of their strong quantum confinement, due to the large exciton Bohr radius of both electrons and holes (18 nm) [17]. Producing PbS thin films on silicon substrates is important because this provides a means for integration of it into electronic devices. PbS/Si heterojunction has been widely used in optoelectronic devices, in which the Si is used as substrate and PbS film as IR absorbent layer [18]. A few reports about the PbS-based heterostructures have been made for photocatalytic applications [19, 20]. The quality of the PbS/nanostructured Si/Si interface plays an important role in the transport of this charge carrier from the PbS to Si surface. Unfortunately, direct growth of PbS onto silicon substrates has been a problem. It was reported that lattice mismatch of reaching 9% exists [21]. Employing buffer layers can

✉ S. Kaci
kacisamirahdr@gmail.com; k_samira05@yahoo.fr

[1] Thin Films Surfaces and Interfaces Division, CMSI-CRTSE, Research Center on Semiconductor Technology for Energetic, 2BD Frantz Fanon, POB 140, 7 merveilles, Algiers, Algeria

[2] Laboratory of Applied Chemistry and Chemical Engineering, Sciences Faculty, LCAGC-UMMTO, Mouloud Mammeri University of Tizi Ouzou, Tizi Ouzou, Algeria

eliminate the problem. Porous silicon has been utilized as a buffer between a Si substrate [22–24]. Nanostructured silicon buffer layer were also employed for designing Si Based photocathodes for PEC CO_2 reduction [25, 26]. Lot of studies investigated the use of PbS/Si in many applications [27–29]. Hence, no studies reported the use of PbS/Si for PEC reduction of CO_2. Hence, in this work, PbS thin film on Si modified surface by pyramidat texturation were prepared by combination of double aqueous chemical etching of silicon substrates followed by chemical bath deposition of nanostructured PbS thin films in order to evaluate their photocatalytic activity for CO_2 reduction. Previous studies demonstrated that the photoelectrocatalytical property of the Si-based electrodes was greatly affected by the surface structures and that of nanostructured Si electrodes were more effective than flat Si electrode for water reduction [30]. Our study was motivated by the fact that the silicon surfaces sensitized by PbS nanoparticles in this way could enhance the absorption of visible-NIR wavelenghs and hence could efficiently act as photocatalyst for PEC CO_2 reduction to value added products. We also predict that the SiPYs modified by PbS could achieve an improvement in photoelectrocatalytic activity towards PEC reduction of CO_2.

1.1 Experimental Procedure

The pyramidale texturation of the monocrystalline silicon sample surface was carried out in KOH aqueous solution. The monocrystalline silicon samples were (100) oriented, p-doped with resistivity about 1 Ω ~ 10 Ω. The size is about 1.5×1.5 mm^2. Before etching, the samples were successively immersed in acetone then ethanol in ultrasonic clearing machine for 10 min to remove impurity. Then, they have been rinsed with flowing deionized water. After rinsing, the samples were dried under a stream of dry N_2. The cleaned samples were textured in an alkaline mixture solution consisting of KOH + IPA (isopropyl alcohol) + H_2O at T = 85 °C for 15 min. Then, the samples were rinsed with deionized water and dried with dry N_2 flow [31].

PbS thin films were prepared by following the deposition bath steps described previously [32].

The photoelectrochemical performance of PbS/Si(100) and PbS/SiPYs/Si(100) samples was evaluated through linear sweep voltammetry (LSV) and cyclic voltammetry using an AUTOLAB potentiostat with a conventional three electrodes setup. The parameters were chosen so as to conduct the CO_2 conversion in the simplest and practice way, hence, we have carried out the experiences at normal conditions of temperature and pressure. The photocatalyst was supported on silicon wafer since this later is the better material used in solar collector. The electrolyte used was a solution of K_2CO_3, it is frequently used as CO_2 source, but also ensures an alkaline medium which favores the CO_2 conversion and suppresses as possible the H_2 evolution. For these electrochemical purposes, the PbS thin films, deposited onto Si(100) and SiPYs modified Si(100) substrates, were used as working electrode (with an effective area of $3cm^2$); Ag/AgCl (3.5 M KCl) as reference and Pt rod as counter electrode. The electrolyte was 0.01 M K_2CO_3 solution. In order to calculate the flat band potential (E_{fb}) of the films in the range from −1.5 to 0.5 V vs Ag/AgCl (3.5 M KCl), we conducted the electrochemical measurments in dark and under artificiel visible light delivred by lamp with power of 70 W. The CO_2 reduction reaction (CO_2RR) measurements were performed in an airtight one compartment electrochemical cell under ambient temperature and solar room lightning as it was shown in Fig. 1. The compartment consisted of PbS/SiPYs/Si as the working electrode, SCE as the reference electrode and the platinum wire as the counter electrode. 0.01 M aqueous K_2CO_3 was used as the electrolyte and was saturated with CO_2 during 30 min which was generated artisanally by making mixtures of (sugar+baking powder+warming water). The generated CO_2 gas was bubbled into water continuously with a uniform velocity (10 sccm). The photoelectrocatalytic measurements were carried out by speaping the potential from −1.5 V to +1.5 V for 1 h (10 cycles). The liquid phase products were analysed by a GC measurments. The samples were analyzed using Gas Chromatography equipped with a thermal conductivity detector.

Fig. 1 Experimental Set-up of PEC reduction of CO_2

2 Results and Discussion

2.1 Formation and Morphology of Pyramidal Silicon and PbS Deposition

Figure 2 shows a schematic model of (100) surface etching with NaOH concentration. At the beguining, Si–OH bond are formed resulting from the interaction of OH^- ions produced from hydrolisis of NaOH. After that, dehydration reaction of silicate glass takes place once IPA was added. A vicinal pair are formed by the two unreacted hydroxyls left on the two linked silicon atoms are brought much closer together [33].

Figure 3a shows the SEM micrograph of the prepared Si pyramids textured surface (SiPYs). The pyramids are randomly distributed over the whole surface of the sample. Different pyramids sizes are apparent as shown in Fig. 3a. Figure 4b shows the SEM image of the PbS nanocrystalline thin film prepared on the SiPYs/Si(100) substrate by the CBD method. The PbS nanoparticles cover the whole surface of the SiPYs surface (Fig. 3b and c).

2.2 Surface Reflectance Measurments

The surface reflectance of the different silicon samples is given in Fig. 4a Over the measured interval (400–2000 nm) of wavelengths.

The reflectance of pyramids textured surface is significantly lower than the reflectance of the non textured surface. The reflectance of the pyramids textured surface is lower especially at longer wavelengths. The decrease of the reflectance insinuates that a sunlight absorption improvement will be occured. The reflectance of PbS sensitized flat silicon

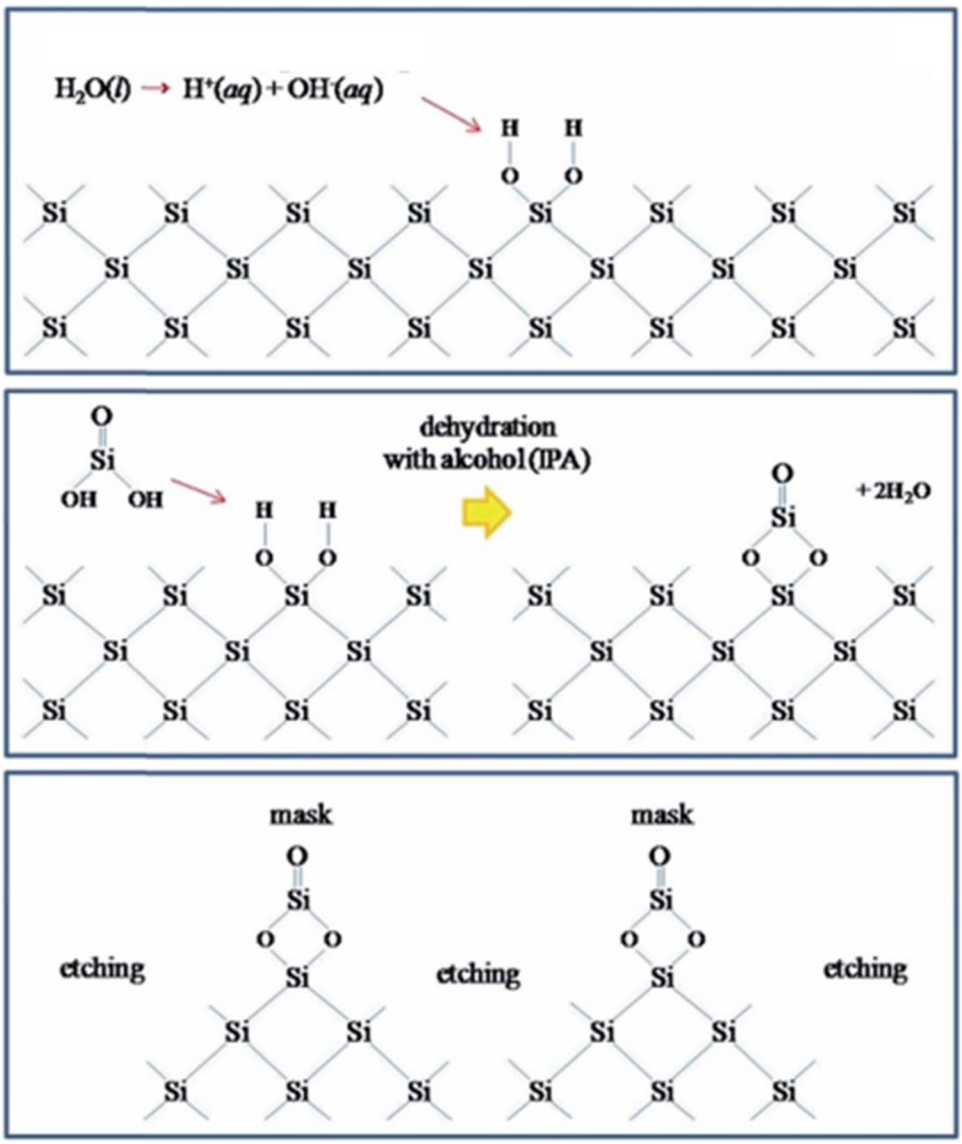

Fig. 2 Illustration of Si surface pyramidal texturation with KOH [33]

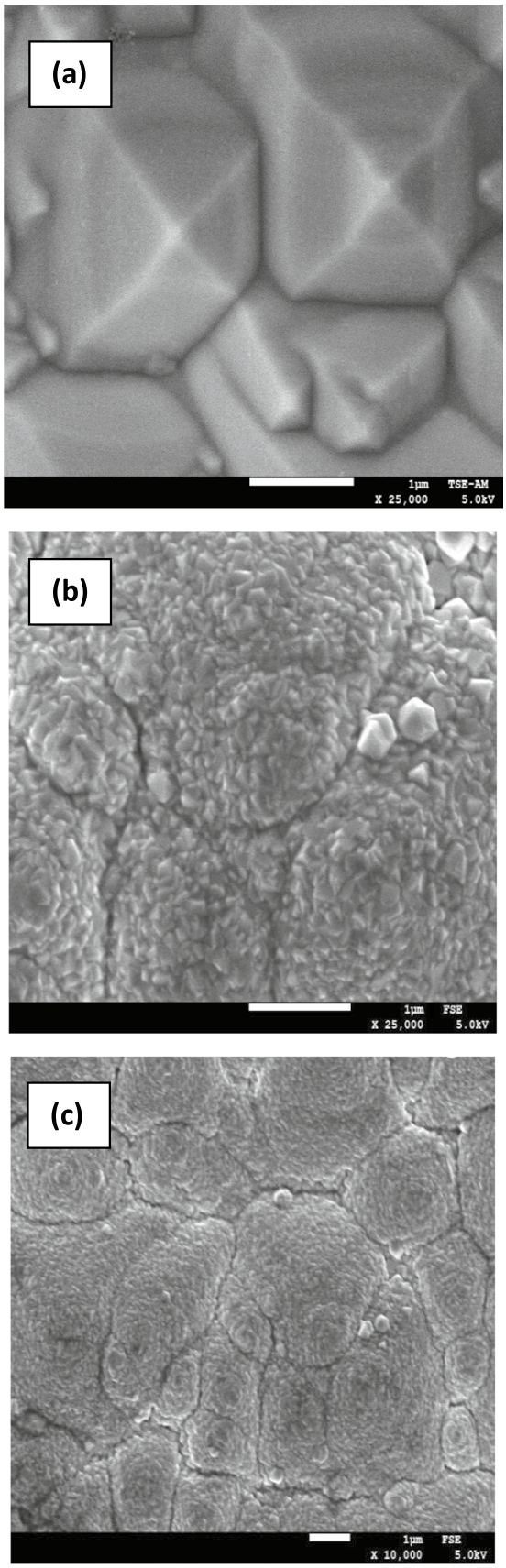

Fig. 3 SEM observations of SiPYs modified Si(100) substrates (**a**) before and (**b**, **c**) after PbS thin film deposition

sample is given in Fig. 4b. It is clear that the sensitization with PbS nanoparticles enhance the optical absorption at longer wavelengths and depended on the surface morphology of the silicon samples. The optimized reflectance of the samples with pyramids textured surface single out this approach as very attractive photocathode with enhanced functionality for solar driven PEC reduction either of water or CO_2.

It is known that flat silicon light's absorption is limited to visible range of the solar spectrum. Hence, by structuring its surface, either by pyramidal texturation or by producing nanowires, a broad range of solar wavelengths can be absorbed as it is shown in the Fig. 4a, in which the reflectivity of the silicon surface decreased drastically after pyramidal texturation compared to the non-treated surface which means that the light absorption of the silicon surface has increased (see Fig. 5). This absorption is further observed

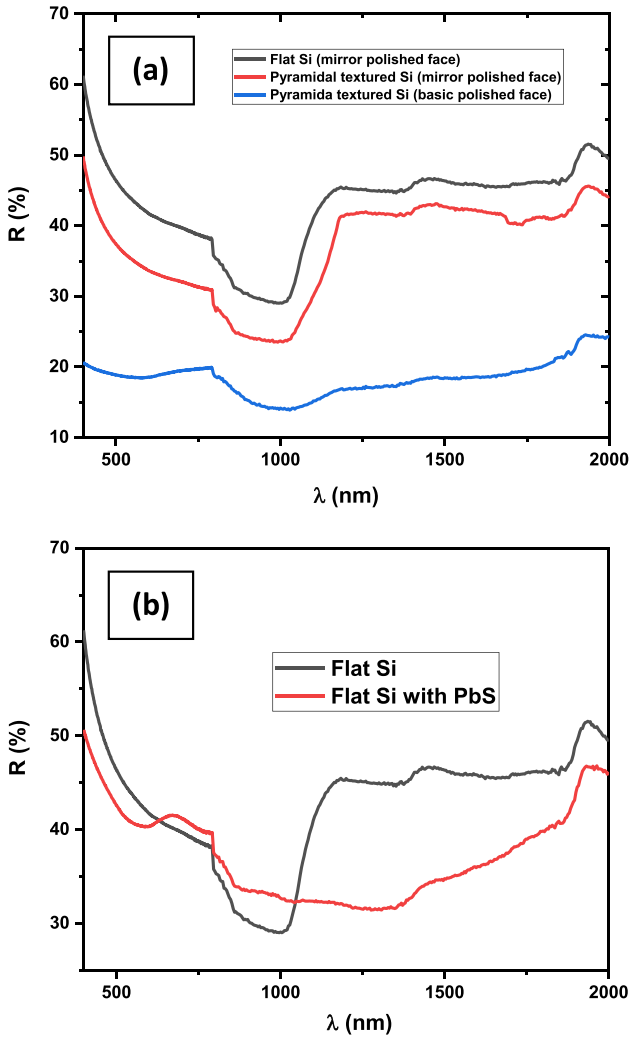

Fig. 4 Reflection spectra (**a**) after pyramids texturation and (**b**) sensitization with PbS

Fig. 5 Light-matter interaction on planar Si and Si pyramids

when a basic polished silicon is used, which indicates that the formation of pyramids is sensitive to surface roughness and this later is more suitable for producing pyramids.

We have used the diffuse reflectance of the PbS/Si to determine the band gap energy of PbS thin film which was estimated, employing the Kabulka Munk relation [34] to be equal to 0.56 eV. Regarding what was reported in previous studies, the mean grain size of PbS particles corresponding to 0.56 eV is about 10 nm [19]. The relationship between the band-gap of PbS QDs and particle size is summurized in the Fig. 6. We found the type of conductivity of the deposited PbS thin film electrochemicaly by carrying LSV of a PbS sample in dark and under illumination.

2.3 Energy Diagram and Band Position of PbS/Si

An attempt to construct the band diagram energy of the studied heterostructure was undertaken. A pellet was made from PbS nanopowder obtained at the end of the PbS thin film deposition from the chemical bath by filtration of the resulting solution.

The increase of the photocurrent I_{ph} along the positive polarization (Fig. 7) is consistent with n-type conductivity.

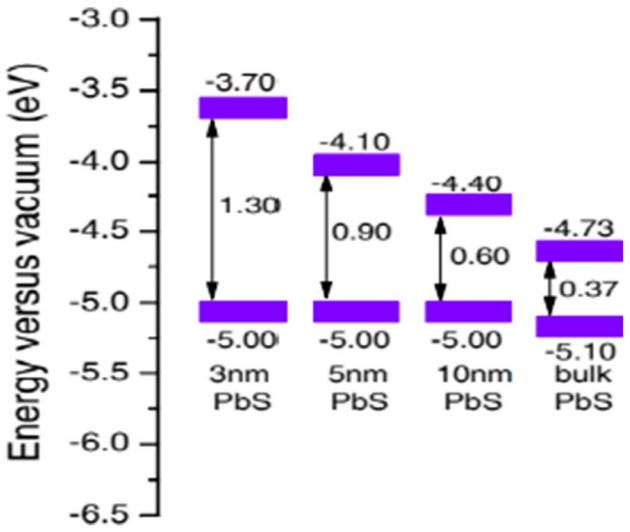

Fig. 6 Evolution of the band-gap of PbS with particle size [19]

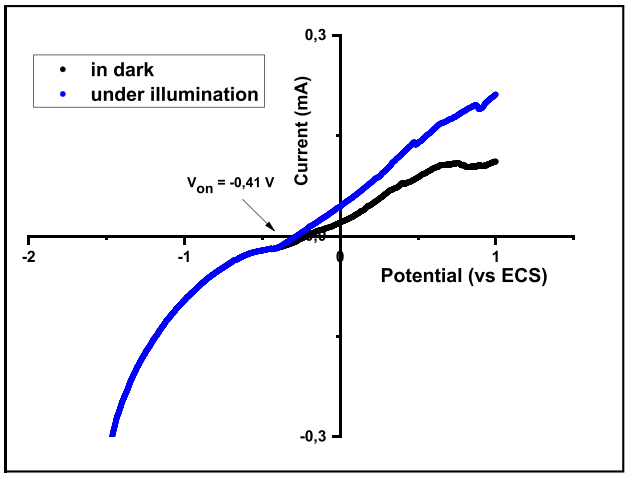

Fig. 7 LSV curve of PbS pellet in aqueous KOH solution (0.1 M)

The linear plot of I_{ph}^2 intercept the potential axis gives the flat band potential E_{fb} [35]. The energies of the valence (EVB) and conduction bands (ECB) of a material are of great importance in applied photocatalysis and valuable information can be extracted from the PEC characterization. Their knowning allows the energy diagramm construction of the different band energy position of the studied material. They can be detrmined using the following relations:

$$ECB = -4.75 + e\,V_{fb} + E_a$$
$$EVB = ECB - E_g$$

where −4.75 eV represents the potential of the referenc electrode (SCE) vs vacuum and E_a is the activation energy which is the difference between conduction bande and Fermi level. For E_g of 0.56 eV and neglicting the E_a, we found: ECB = −4.54 eV et EVB = −5.10 eV.

These values indicat that the conduction bande (BC) derives principally from orbitale *6 s* of lead while the valence bande consists of the orbitale *3 s* of sulfur and the optical transition is attributed to the charge transfert S^{2-}: *3 s* → Pb^{2+}: *6 s*.

As can be seen from Fig. 8, the Si valence band edge is obviously below the PbS band edge, which satisfies the energetic requirement for hole transfer. Moreover, the canduction band is higher than that of PbS, hence, for contact formation, the electrons will be transferred from the Si to PbS until a thermodynamic equilibrium is established. An electron depletion region and surface high level band will result in Si to facilitate electron and hole transfer.

2.4 Photoelectrocatalytic Properties

The photoelectrocatalytic properties were first tested towards water reduction in absence of CO_2. The Fig. 9 shows the LSV tests for the two PbS/SiPYs/Si based

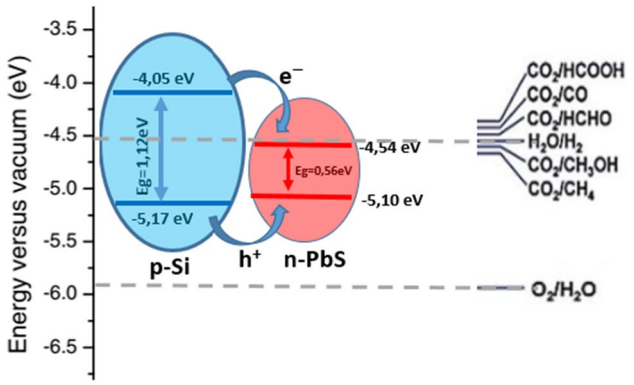

Fig. 8 Energy diagram illustrating the band energy positions of PbS/Si heterostructure

working electrodes, in dark and under artificial visible light, for different SiPYs samples. As can be seen, at -1 V vs Ag/AgCl (the theoretical potential necessary for water reduction), the generated cathodic photocurrent for the SiPYs/Si(100) in dark is negligible compared with the cathodic photocurrent of PbS/SiPYs/Si(100) based electrode, which was significantly enhanced by the synergy between the PbS nanoparticles and SiPYs to generate the charge carriers for reduction of water molecule. Additionally, the photocurrent of PbS/SiPYs/Si(100), which pyramides were obtained on silicon miror polished face, was improved with respect to that obtained on silicon basic polished face, which means that the electron-hole transport to the surface was improved. The fact that PbS/SiPYs/Si structure disposes of a broad range of the light spectrum explain the above observation, as was attested by the reflectance spectra.

From these results, it is possible to photoelectrochemically reduce carbon dioxide to methanol and or formate, even if carbon dioxide's reduction to methanol potential is only 20 mV positive of water reduction, which compete the CO_2RR by hydrogen generation. Therefore, the studied working electrodes based on PbS/SiPYs/Si have a high hydrogen overpotential which allows the reduction reaction of carbon dioxide to achieve high selectivity and rates well before water reduction occurs.

2.5 Investigations of PbS/SiPYs/Si Photocathodes for CO_2 Reduction Reaction

The cyclic voltammograms (CVs) of the PbS/SiPYs/Si are shown in Fig. 10. Under CO_2 saturated conditions (pH = 10), a distinct oxidation peak is observed on the prepared electrode, in the first anodic scan, indicating the oxidation of PbS to $Pb_{1-x}S$ [36] as was given by the following equation:

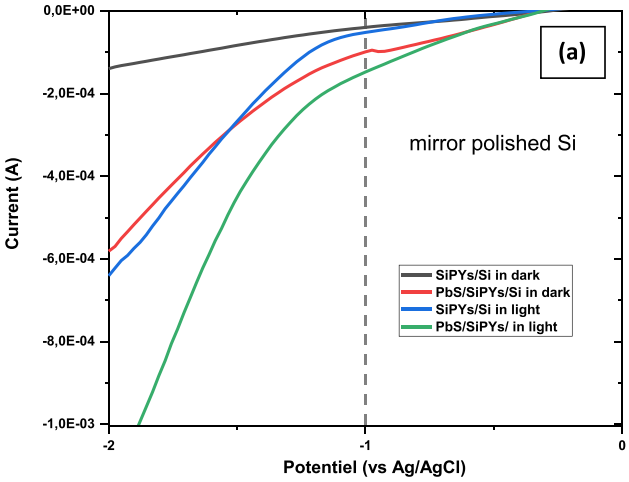

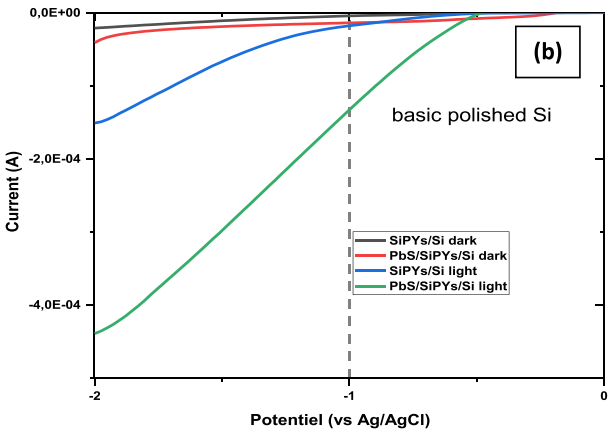

Fig. 9 LSV of SiPYs/Si(100) and PbS/SiPYs/Si(100) based working electrodes, as function of surface polishing type in dark and under illumination in 10^{-2} aqueous K_2CO_3

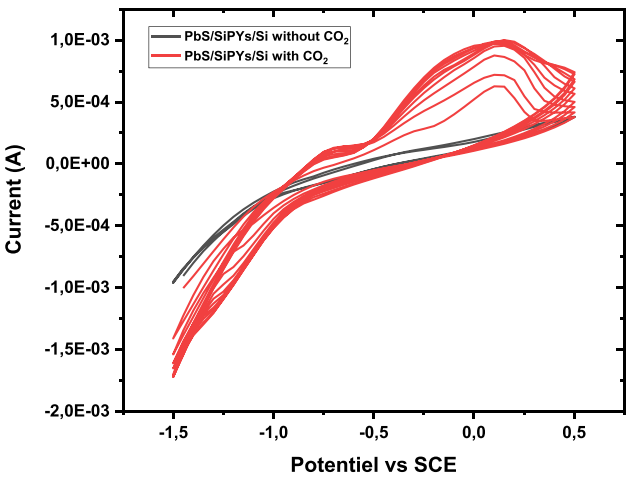

Fig. 10 Cyclic voltammograms (10 mV/s) of a freshly prepared PbS/SiPYs/Si photocathode in 0.01 M K_2CO_3 under light and after 30 min of CO_2 bubbling which show the successful reduction of CO_2

$$2PbS + 3H_2O + 2CO_3^{2-} \rightarrow 2PbCO_3 + 6H^+ + 8e^- + S_2O_3^{2-} \ (E^\circ = +0.220\ V\ vs\ SHE) \quad (1)$$

A formation of a metastable sulfur-rich sulfide underlayer is supposed to occur at the initial oxidation stage, yielding a monolayer of $PbCO_3$ in alkaline solutions [36]. It was noticed that the oxidation peak was observed after bubbling the solution with CO_2, indicating that the oxidation of PbS particles was influenced by the presence of CO_2 or CO_3^{2-}/HCO_3^-. Other peaks were observed and seem to be kept in the same position in the following scans. Also, an enhanced cathodic current is observed at potentials ≤ −0.6 V (vs. SCE electrode), which demonstrates that the CO_2 is effectively reduced [37]. Also the influence of PbS particles was evidenced through the enhancing the photocatalytic activity of the photocathode after decorating SiPYs with the sulfide. Hence, it was observed in Fig. 8 the shifting towards the positive potential after addition of CO_2. An enhancing of 200 mV was noticed which confirm the photocatalytic activity of the working electrode toward CO_2.

As seen in this figure, CH_3OH evolution increased with an increase in the applied potential, the tendency of which corresponded to the increase of the photocurrent response of the photocathode which occured from the photoelectrochemical reduction of CO_2 to CH_3OH. The thermodynamic potential for photoelectrochemical reduction of CO_2 to CH_3OH in the presence of protons is generally explained by the following equation:

$$CO_2 + 6\,e^- + 6H^+ \rightarrow H_2O + CH_3OH\ E^\circ = -0.62\ V\ vs\ SCE\ (-0.38V\ vs\ SHE) \quad (2)$$

A lead atom layer could be achieved through the electrochemical oxidation of PbS during CO_2RR, due to the presence of positive oxidation state(s) of Pb centers, simultaneously with the ease of chalcogenide anions removal in aqueous solutions [37]. Previous studies reported that during photoelectrocatalysis, the nanocrystalline PbS were reduced into Pb and demonstrated that during the PbS-to-Pb transformation, $PbCO_3$ phase results from the anion exchange equilibrium: S^{2-} / HCO_3^- / CO_3^{2-}, and being the principal source to bring out the Pb thin films formation [38]. The Fig. 11 shows the EDS analysis and the SEM of the surface of the working electrode used for CO_2RR at the end of the reaction, we can see that the sulfur « S » element desapeared and one can only see the lead « Pb » element, which means that the PbS was effectively turned to Pb during the CO_2RR. Some carbon element atoms were detected on the surface, which suppots the results previously reported in ref. [38].

Other explanation regarding the photogenerated-hole-induced instability of metal sulfides must be taken into the account. Indeed, upon suitable light illumination, a generation of electrons and holes from the conduction band (CB)

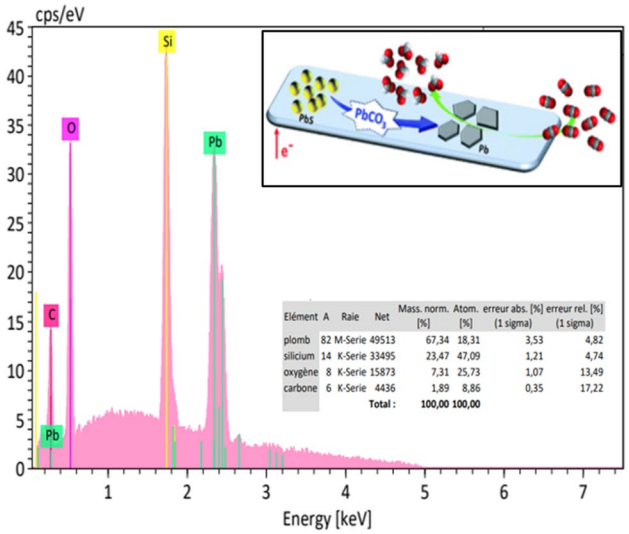

Fig. 11 EDX analysis of the surface of the working electrode PbS/SiPYs/Si after CO_2RR

and valence band (VB), in the mentioned order. Photoexcited electrons passe to the surface while the transfer of holes is poses problem. An outer surface enrichment by the photogenerated holes takes place on of the metal sulfide photocatalyst waiting for being consumed by electron donors in the reaction system. Under similar conditions, photocorrosion has frequently been observed originating from irreversible hole-driven oxidation reactions in metal sulfides, driving to the oxidation of surface sulfide ions (S^{2-}) to sulfur (S^0) and/or sulfate ($S_2O_3^{2-}$), thereby resulting in low photostability of metal sulfides that greatly restricts their practical applications. Therefore, the accumulation of excess photoinduced holes on the metal sulfide surface is the main cause of photodissolution [39]. Figure 12 shows the characteristic peaks of a Gas Chromatograph for the the electrolyte before and after CO_2RR and for the pure Methanol which was used as standard to allow the different concentration calculations. As we can see, a methanol was detected as one of the most product between the multiple other products of CO_2RR in very small concentrations compared to that of methanol. This is in adequacy regarding the constructed energy diagram of band energy positions of Si and PbS in which, the BC of PbS was well positionned to allow the reduction of CO_2 to methanol instead of other products, and the electron transfert rised by the enhanced light absorption of silicon nanowires makes the reduction easy thanks to the availability of sufficient electron to allow the transformation of CO_2 to Methanol following the Eq. 2.

The consumption of electrons during the reduction of CO_2 is associated by the utilization of produced holes for anodic oxidation of PbS to $PbCO_3$, hence, the photocorrosion is avoided and a thin film of Pb is produced on the

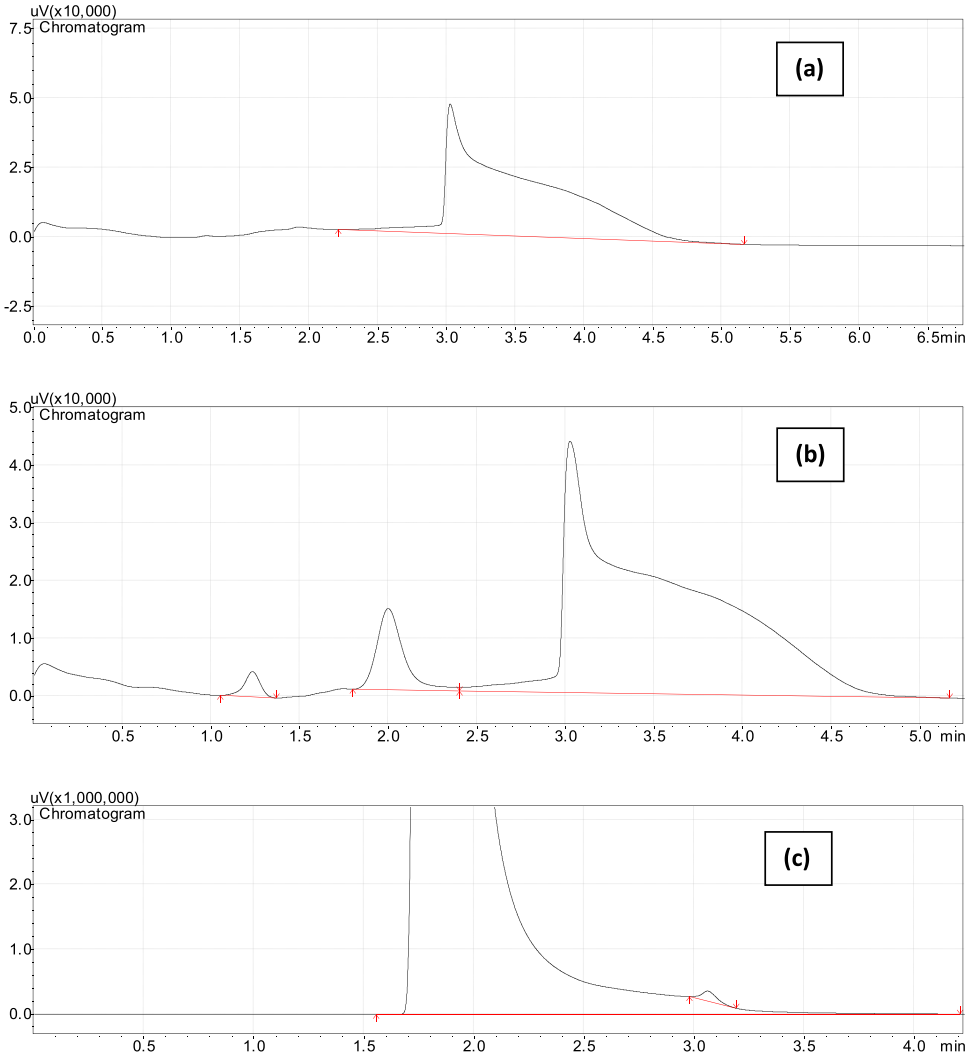

Fig. 12 Characteristic peaks of a Gas Chromatograph of (**a**) Electrolyte before CO_2 reduction, (**b**) Electrolyte after CO_2 reduction and (**c**) pure methanol. Approximate peak time for Methanol: 2 min

surface of the SiPYs which plays itself the role of electrocatalyst as explained previously. The electrode based on PbS/SiPYs/Si could be used as photocathode for the PEC reduction of CO_2.

3 Conclusions

In this work, a working electrode based on coupling PbS thin films on SiPYs/Si substrates were applied as photocathode in both water splitting and CO_2 reduction reaction. The band gap energy of PbS was 0.56 eV which means that the obtained PbS particles were nanocristallines. The impact of introducing the PbS nanoparticles was well established and evidenced. It was shown that the performance toward water reduction of the photocathodes was influenced by the polishing nature of the silicon substrate on which SiPYs structures were formed. The SiPYs obtained on miror plished face exhibited the best water reduction. The CO_2 photoelectrocatalytic test showed that the PbS thin film on SiPYs/Si exhibits a higher CO_2 reduction in comparison with the flat Silicon. An effective separation of the charge carrier and their transport to the surface due to suitable positions of energy bands were verified by the band diagram of energy position of the PbS/Si. It was concluded that $PbCO_3$ film was formed on the surface of the SiPYs avoiding by this the photocorrsion of the surface. Methanol was the main product produced from the CO_2RR confirming by the way the applicability of the PbS/SiPYs/Si based photocathode for PEC reduction of CO_2. In addition, the direct oxidation of nanocrystalline PbS could be a good method for direct preparation of d-orbital-filled Pb nanocrystals. The oxidation of PbS to Pb is not a drawback since nanocrystalline Pb consists one of the universal electrocatalyst to produce formic acid as a primary product of CO_2RR in aqueous electrolytes.

Acknowledgments The authors gratefully acknowledge the financial support from the Directorate General for Scientific Research and Technological Development (DGRSDT-Algeria).

Authors' Contribution L. Allad: Methodology, Experimental investigations. S. Kaci: Supervisor, Validation, Data curation. K. Benfadel: Investigations. D. Allam: Characterization. A. Ouerk: Methodology. A. Boukezzata: Investigations. C. Torki: Methodology, Investigations. S. Anas: Investigations. L. Talbi: Investigations. Y. Ouadah: Investigations. S. Hocine: Characterizations. A. Keffous: Investigations. S. Achacha: Characterization. A. Manseri: Characterization. S. Sam: Characterization.

Data Availability My manuscript and associated personal data.

Declarations

Ethics Declarations The manuscript has not been published.

Research Involving Human Participants and/or Animals Not applicable' for that section.

Informed Consent Not applicable' for that section.

Consent to Participate The authors consent to participate.

Consent for Publication The author's consent for publication.

Declaration of Competing Interest The authors declare that they have no known competing financial interests.

Conflict of Interest The authors declare that they have no conflict of interest.

References

1. Cheng J, Zhang M, Wu G, Wang X, Zhou J, Cen K (2014) Photoelectrocatalytic reduction of CO_2 into chemicals using Pt-modified reduced graphene oxide combined with Pt-modified TiO_2 nanotubes. Environ Sci Technol. https://doi.org/10.1021/es500364g
2. Xie S, Zhang Q, Liu G, Wang Y (2016) Photocatalytic and photoelectrocatalytic reduction of CO_2 using heterogeneous catalysts with controlled nanostructures. Chem Commun. https://doi.org/10.1039/C5CC07613G
3. Chen P, Zhang Y, Zhou Y, Dong F (2021) Photoelectrocatalytic carbon dioxide reduction: fundamental, advances and challenges. Nano Mat Sci. https://doi.org/10.1016/j.nanoms.2021.05.003
4. Wang L, Wei Y, Fang R, Wang J, Yu X, Chen J, Jing H (2020) Photoelectrocatalytic CO_2 reduction to ethanol via graphite-supported and functionalized TiO_2 nanowires photocathode. J Photochem Photobiol A Chem. https://doi.org/10.1016/j.jphotochem.2020.112368
5. Ueda Y, Takeda H, Yui T, Koike K, Goto Y, Inagaki S, Ishitani O (2015) A visible-light harvesting system for CO_2 reduction using a Ru(II) -re(I) photocatalyst adsorbed in mesoporous organosilica. Chem Sus Chem. https://doi.org/10.1002/cssc.201403194
6. Yadav RK, Lee JO, Kumar A, Park NJ, Yadav D, Kim JY, Baeg JO (2018) Highly improved solar energy harvesting for fuel production from CO_2 by a newly designed graphene film Photocatalyst. Sci Rep. https://doi.org/10.1038/s41598-018-35135-7
7. Proppe AH, Li YC, Guzik AA, Berlinguette CP, Chang CJ, Cogdell R, Doyle AG, Flick J, Gabor NM, van Grondelle R, Schiffer SH, Jaffer SA, Kelley SO, Leclerc M, Leo K, Mallouk TE, Narang P, Schlau-Cohen GS, Scholes GD et al (2020) Bioinspiration in light harvesting and catalysis. Nat Rev Mater. https://doi.org/10.1038/s41578-020-0222-0
8. Xie B, Lovell E, Hao Tan T, Jantarang S, Yu M, Scott J, Amal R (2021) Emerging material engineering strategies for amplifying photothermal heterogeneous CO_2 catalysis. J Ener Chem. https://doi.org/10.1016/j.jechem.2020.11.005
9. Mo Y, Wang C, Xiao L, Chen W, Lu W (2021) Artificial light-harvesting 2D photosynthetic system with iron phthalocyanine/graphitic carbon nitride composites for highly efficient CO_2 reduction. Catal Sci Technol. https://doi.org/10.1039/D1CY00858G
10. Zhang N, Long R, Gao C, Xiong Y (2018) Recent progress on advanced design for photoelectrochemical reduction of CO_2 to fuels. Sci China Mater. https://doi.org/10.1007/s40843-017-9151-y
11. LaTempa TJ, Rani S, Bao N (2012) Generation of fuel from CO_2 saturated liquids using a p-Si nanowire‖n-TiO2 nanotube array photoelectrochemical cell. Nanoscale. https://doi.org/10.1039/c2nr00052k
12. Beeman JW, Bullock J, Wang H, Eichhorn J, Towle C, Javey A, Toma FM, Mathews N, Ager JW (2019) Si photocathode with ag-supported dendritic cu catalyst for CO_2 reduction. Ener Env Sci. https://doi.org/10.1039/C8EE03547D
13. Ding P, Hu Y, Deng J, Chen J, Zha C, Yang H, Han N, Gong Q, Li L, Wang T, Zhao X, Li Y (2019) Controlled chemical etching leads to efficient silicone bismuth interface for photoelectrochemical CO_2 reduction to formate. Mater Today Chem. https://doi.org/10.1016/j.mtchem.2018.10.009
14. Hu YP, Chen FJ, Ding P, Yang H, Chen JM, Zha CY, Li YG (2018) Designing effective Si/ag interface via controlled chemical etching for photoelectrochemical CO_2 reduction. J Mater Chem A. https://doi.org/10.1039/C8TA05420G
15. Choi SK, Kang U, Lee S (2014) Sn-coupled p-Si nanowire arrays for solar formate production from CO_2. Adv Ener Mater. https://doi.org/10.1002/aenm.201301614
16. Dasog M, Kraus S, Sinelnikov R, Veinot JGC, Rieger B (2017) CO_2 to methanol conversion using hydride terminated porous silicon nanoparticles. Chem Comm. https://doi.org/10.1039/C7CC00125H
17. Kaci S, Keffous A, Trari M, Menari H, Manseri A, Mahmoudi B, Guerbous L (2010) Influence of polyethylene glycol-300 addition on nanostructured lead sulfide thin films properties. Opt Comm. https://doi.org/10.1016/j.optcom.2010.04.046
18. Bashkany ZA, Abbas IK, Mahdi MA, Al-Taay HF, Jennings P (2018) A self-powered heterojunction photodetector based on a PbS nanostructure grown on porous silicon substrate. Silicon. https://doi.org/10.1007/s12633-016-9462-4
19. Du K, Liu G, Chen X, Wangz K (2015) PbS quantum dots sensitized TiO_2 nanotubes for photocurrent enhancement. J Electrochem Soc. https://doi.org/10.1149/2.0661510jes
20. Carrasco-Jaim OA, Ceballos-Sanchez O, Torres-Martínez LM, Moctezuma E, Gómez-Solís C (2017) Synthesis and characterization of PbS/ZnO thin film for photocatalytic hydrogen production. J Photochem Photobio A Chem. https://doi.org/10.1016/j.jphotochem.2017.07.016
21. Shaban M, Rabia M, Abd El-Sayed AM, Ahmed A, Sayed S (2017) Photocatalytic properties of PbS/graphene oxide/polyaniline electrode for hydrogen generation. Sci Rep. https://doi.org/10.1038/s41598-017-14582-8
22. Zhong H, Mirkovic T, Scholes GD (2011) Nanocrystal synthesis. Comp Nanosci Tech. https://doi.org/10.1016/B978-0-12-374396-1.00051-9
23. Popov G, Bačić G, Mattinen M, Manner T, Lindström H, Seppänen H, Suihkonen S, Vehkamäki M, Kemell M, Jalkanen P, Mizohata K, Räisänen J, Leskelä M, Koivula H, Barry ST, Ritala

M (2020) Atomic layer deposition of PbS thin films at low temperatures. Chem Mater. https://doi.org/10.1021/acs.chemmater.0c01887
24. Rahmani N, Dariani RS, Rajabi M (2016) A proposed mechanism for investigating the effect of porous silicon buffer layer on TiO_2 nanorods growth. Appl Surf Sci https://www.cheric.org/research/tech/periodicals/doi.php?art_seq=1453525
25. Taherkhani M, Naderi N, Fallahazad P, Javad Eshraghi M, Kolahi A (2019) Development and optical properties of ZnO Nanoflowers on porous silicon for photovoltaic applications. J Electron Mater. https://doi.org/10.1007/s11664-019-07484-0
26. Kong Q, Kim D, Liu C, Yu Y, Su YD, Li YF, Yang PD (2016) Directed assembly of nanoparticle catalysts on nanowire photoelectrodes for photoelectrochemical CO_2 reduction. Nano Lett. https://doi.org/10.1021/acs.nanolett.6b02321
27. Kaci S, Keffous A, Hakoum S, Trari M, Mansri O, Menari H (2014) Preparation of nanostructured PbS thin films as sensing element for NO_2 gas. Appl Surf Sci. https://doi.org/10.1016/j.apsusc.2014.03.190
28. Kaci S, Keffous A, Hakoum S, Manseri A (2015) Hydrogen sensitivity of the sensors based on nanostructured lead sulfide thin films deposited on a-SiC: H and p-Si (100) substrates. Vacuum. https://doi.org/10.1016/j.vacuum.2015.02.024
29. Kaci S, Keffous A, Trari M, Mahmoudi B, Menari H (2011) Enhancement of Blue Spectral Response Intensity of PbS via Polyethylene Oxide-Adding for the Application to White LEDs. Adv Mater Res. https://doi.org/10.4028/www.scientific.net/AMR.227.39
30. Dimitrova DZ, Du CH (2013) Crystalline silicon solar cells with micro/nano texture. Appl Surf Sci. https://doi.org/10.1016/j.apsusc.2012.10.081
31. Kaci S, Rahmoune R, Kezzoula F, Boudiaf Y, Keffous A, Manseri A, Menari H, Cheraga H, Guerbous L, Belkacem Y, Chalal R, Bozetine I, Boukezzata A, Talbi L, Benfadel K, Ouadfel MA, Ouadah Y (2018) Impact of porous SiC-doped PVA based LDS layer on electrical parameters of Si solar cells. Opt Mater. https://doi.org/10.1016/j.optmat.2018.05.006
32. Kaci S, Keffous A, Hakoum S, Makrani N, Kechouane M, Guerbous L (2012) Investigation of nc-PbS/a-$Si_{1-x}Cx$: H/pSi (1 0 0) heterostructures for LED applications. Opt Mater. https://doi.org/10.1016/j.optmat.2012.05.031
33. Ju M, Balaji N, Park C, Thi Thanh Nguyen H, Cui J, Oh D, Jeon M, Kang J, Shim G, Yi J (2016) The effect of small pyramid texturing on the enhanced passivation and efficiency of single c-Si solar cells. RSC Adv. https://doi.org/10.1039/c6ra05321a
34. Hecht HG (1976) The interpretation of diffuse reflectance spectra. J Res Nat Bur Stand-A Phys Chem. https://doi.org/10.6028/jres.080A.056
35. Kuhl KP, Cave ER, Abram DN, Jaramillo TF (2012) Energy Environ Sci. https://doi.org/10.1039/C2EE21234J
36. Chernyshova IV (2001) Anodic oxidation of galena (PbS) studied FTIR-Spectroelectrochemically. J Phys Chem B. https://doi.org/10.1021/jp0110253
37. Gao MR, Xu YF, Jiang J, Yu SH (2013) Nanostructured metal chalcogenides: synthesis, modification, and applications in energy conversion and storage devices. Chem Soc Rev. https://doi.org/10.1039/C2CS35310E
38. Zhang Z, Liu C, Brosnahan JT, Zhou H, Xu W, Zhang S (2019) Revealing structure evolution of PbS nanocrystal catalysts in the electrochemical CO_2 reduction using in situ synchrotron radiation X-ray diffraction. J Mater Chem A. https://doi.org/10.1039/C9TA06750G
39. Weng B, Qi MY, Han C, Tang ZR, Xu YJ (2019) Photocorrosion inhibition of semiconductor-based Photocatalys: basic principle, current development, and future perspective. ACS Catal. https://doi.org/10.1021/acscatal.9b00313